

**The Optical Gravitational Lensing Experiment.  
The Catalog of Stellar Proper Motions toward the Magellanic Clouds<sup>1</sup>**R. Poleski<sup>1</sup>, I. Soszyński<sup>1</sup>, A. Udalski<sup>1</sup>,  
M. K. Szymański<sup>1</sup>, M. Kubiak<sup>1</sup>, G. Pietrzyński<sup>1,2</sup>,  
Ł. Wyrzykowski<sup>1,3</sup> and K. Ulaczyk<sup>1</sup><sup>1</sup>Warsaw University Observatory, Al. Ujazdowskie 4, 00-478 Warszawa, Poland  
e-mail: (rpoleski,soszynsk,udalski,msz,mk,pietrzyn,wyrzykow,kulaczyk)@astrouw.edu.pl<sup>2</sup>Universidad de Concepción, Departamento de Astronomia, Casilla 160-C, Concepción,  
Chile<sup>3</sup>Institute of Astronomy, University of Cambridge, Madingley Road, Cambridge CB3  
0HA, UK*Received February 8, 2012*

## ABSTRACT

We present a catalog of over 6.2 million stars with measured proper motions. All these stars are observed in the direction of the Magellanic Clouds within the brightness range  $12 < I < 19$  mag. Based on these proper motions about 440 000 Galactic foreground stars can be selected. Because the proper motions are based on a few hundred epochs collected during eight years, their statistical uncertainties are below 0.5 mas/yr for stars brighter than  $I = 18.5$  mag. The parallaxes are derived with uncertainties down to 1.6 mas. For above 13 000 objects parallaxes are derived with significance above  $3\sigma$ , which allows selecting about 270 white dwarfs (WDs). The search for common proper motion binaries among stars presented was performed resulting in over 500 candidate systems. The most interesting ones are candidate halo main sequence star–WD and WD–WD systems. The application of the catalog to the empirically bound Cepheid instability strip is also discussed.

**Key words:** *Astrometry – Catalogs – Stars: kinematics and dynamics – binaries: visual – globular clusters: individual: 47 Tuc*

**1. Introduction**

Proper motions are key parameters for finding intrinsically faint objects and tracing the dynamical properties of the Galaxy. Both of these applications require catalogs containing a large number and uniformly measured proper motions. Most of the existing catalogs of stellar proper motions are based on a small number of

---

<sup>1</sup>Based on observations obtained with the 1.3 m Warsaw telescope at the Las Campanas Observatory of the Carnegie Institution for Science.

epochs separated by at least 10 years (*e.g.*, Fedorov *et al.* 2009, Girardi *et al.* 2011). Here we present a catalog based on a few hundred epochs collected during the third phase of the Optical Gravitational Lensing Experiment (OGLE-III) project. The epochs span over 8-yr time baseline. We analyzed the OGLE-III observations in the directions of the Large and Small Magellanic Clouds (hereafter LMC and SMC; MCs if both are relevant). The OGLE-III survey observed these dense stellar regions with the primary goal to search for possible microlensing events. High stellar density required in order to make the survey efficient, allowed accurate proper motion and parallax determinations. Our catalog can be used in those research areas, where most of the other catalogs of proper motions are less efficient. For the first time the stellar proper motions in the directions of the MCs are explored in such a way.

The stars with proper motions  $\mu \geq 100$  mas/yr were presented separately (Poleski *et al.* 2011, hereafter Paper I). During time baseline of the OGLE-III these stars changed their position by the amount comparable to the seeing of the images. Thus, cross-matching their positions from reference image and distant epoch was harder task and a case-by-case refinement as good as possible was needed to perform on relatively small number of objects (*i.e.*, 551). These objects are also more important from the astrophysical point of view.

Here we focus on common proper motion (CPM) binaries. They are composed of coeval and equidistant stars of the same metallicity, which evolved as single stars. CPM systems can be used to study both the stellar evolution (Monteiro *et al.* 2006, Sesar *et al.* 2008, Catalán *et al.* 2008) and the gravitational potential of the Galaxy (Yoo *et al.* 2004, Quinn *et al.* 2009, Makarov 2012). The other subject which is described in more detail is a search for the non-variable LMC stars located inside the Cepheid instability strip. Our high accuracy geometrically measured parallaxes are used to construct the Hertzsprung-Russell diagram, which allows *e.g.*, selection of white dwarfs (WDs).

Section 2 gives a description of the observations and Section 3 presents how the catalog was prepared. Section 4 describes the data access. We evaluate the properties of the catalog in Section 5 and show in Section 6 how it can be used. A summary is presented in Section 7.

## 2. Observations

The OGLE-III project observed the MCs between 2001 and 2009 with 1.3-m Warsaw telescope, which is situated at the Las Campanas Observatory, Chile. The observatory is operated by the Carnegie Institution for Science. All the observations were collected with the “second generation” camera containing eight  $2048 \times 4096$  CCD chips with  $15 \mu\text{m}$  pixels. The pixel scale was  $0''.26$  and total field of view was  $35' \times 35'.5$ . Only *I* and *V* filters were used and about 90% of observations were secured in the *I*-band. The number of *I*-band epochs varied between 385

and 637 for the LMC fields and between 583 and 762 for the SMC fields with an exception of the field SMC128 for which 1228 epochs were secured. For the present study we used *I*-band images. *V*-band data were used only to provide color information. The total sky area observed was 39.8 square degrees for the LMC fields and 14.2 square degrees for the SMC fields. The sky area observed was within the Galactic coordinates range  $277^{\circ}83 < l < 283^{\circ}87$  and  $-38^{\circ}07 < b < -28^{\circ}49$  for the LMC fields. For the SMC fields the ranges were  $299^{\circ}35 < l < 306^{\circ}36$  and  $-46^{\circ}28 < b < -42^{\circ}14$ . Because of the angular separation of two groups of fields and different Galactic latitudes, in many cases we treat them separately. The details of the instrumentation setup were given by Udalski (2003) while more in-depth description of the observations was given in Paper I.

### 3. Catalog Construction

Most of the published OGLE-III time-series photometry (Udalski *et al.* 2008a) was obtained with the Difference Image Analysis (DIA) method. In the present study we used the time-series astrometry calculated using the DOPHOT software (Schechter *et al.* 1993). The details of the image alignment and the DOPHOT usage were presented by Udalski *et al.* (2008a) and in Paper I. In Paper I we also detailed the procedure of proper motion estimation, which is briefly described below.

Each image taken was spline-resampled to the grid of the reference image of the given field. For the reference images the transformations from pixel coordinates to the equatorial coordinates were derived by comparing positions of bright stars with their 2MASS catalog entries (Skrutskie *et al.* 2006). The proper motions and parallaxes were derived by the least-squares fitting of the observed centroid positions ( $\alpha$ ,  $\delta$ ) to the model defined by the following parameters: proper motion (in right ascension:  $\mu_{\alpha}$  and in declination:  $\mu_{\delta}$ ), parallax ( $\pi$ ), differential refraction coefficient ( $r$ ) and equatorial coordinates for time  $t = 0$  ( $\alpha_0$  and  $\delta_0$ ,  $t = 0$  corresponds to the epoch 2000.0):

$$\alpha(t) = \alpha_0 + \mu_{\alpha}t + \frac{r \sin p \tan z + \pi \sin \gamma \sin \beta}{\cos \delta} \quad (1)$$

$$\delta(t) = \delta_0 + \mu_{\delta}t + r \cos p \tan z + \pi \sin \gamma \cos \beta \quad (2)$$

where  $z$  is the zenith distance,  $\gamma$  is the angular distance to the Sun,  $\beta$  is the angle between the direction of the parallax shift and the direction to the North celestial pole, and  $p$  is the angle between the direction of the refractive shift and the direction to the North celestial pole.

For each exposure the uncertainty of grid fitting was found based on the residuals between the measured positions of bright stars and the positions calculated using the best-fitting models. This uncertainty was square added to the uncertainty of the point spread function fitting (Kuijken and Rich 2002) giving total uncertainty of each position measurement. The reciprocal of the square total uncertainty was

used as a weight in the least-squares fitting. The procedure of fitting parameters was iterative and in each step the observed positions were corrected so that for stars brighter than  $I = 18$  mag the average residua of positions was 0 for a given exposure and the sigma-clipped average proper motion was equal to 0. The dispersion of proper motions for bright stars was used as an estimate of systematic uncertainties (Paper I) and for 95% of subframes was smaller than 0.67 mas/yr per coordinate. The zero point of our proper motion estimates were tied to the LMC, the SMC or 47 Tuc globular cluster (only for field SMC140). The absolute proper motions of the MCs and 47 Tuc were recently discussed by van der Marel *et al.* (2002), Anderson and King (2003), Kallivayalil *et al.* (2006ab) and Piatek *et al.* (2008). We present our measurement of the relative proper motions of 47 Tuc against the SMC in Section 6.3.

Following the Paper I, the value of 1.5 mas was square added to the uncertainties of the parallax measurements. It was found that such a modification of the formal uncertainties was necessary to properly reproduce uncertainties derived on the basis of comparison of stars measured twice – in the overlapping parts of the adjacent fields.

The proper motions and parallaxes were calculated using this procedure for all stars in the OGLE-III MCs fields. We were not able to reliably calculate the proper motions of nearly saturated stars and stars located in the sky very close to them. For the OGLE-III MCs fields the saturation limit is between 11.5 and 12.7 mag in the  $I$ -band and depends mostly on the number density of stars. We removed all objects in the close proximity of stars brighter than  $I = 11.5$  mag. We empirically found a linear relation between  $I$ -band magnitude of bright stars and radius within which stars had to be removed. It was 1' for  $I = 5.9$  mag down to 0' for  $I = 11.5$  mag. For a few brightest stars this radius was found individually. The list of bright stars was taken from the shallow survey of the LMC performed as a part of the OGLE-III project (Ulaczyk *et al.* in preparation) which covered 90% of the LMC fields. For the rest of the LMC and all SMC fields we used stars from the DENIS catalog (Cioni *et al.* 2000). The areas masked decreased the analyzed sky-area by 0.18 and 0.052 square degrees for the LMC and the SMC, respectively (0.005 square degrees in the field SMC140).

Apart from the removal of stars neighboring the very bright ones, special attention was paid to the photometrically variable sources. The changing flux of a variable star produces a shift in the centroid position, if the star is blended. If a detached eclipsing binary is blended, the centroids clump in two groups: one out of eclipse which is closer to the real position of the star, and second, to which points in the eclipse belong, much more affected by blending. For some binaries which are heavily blended and have a small number of points in ingress and egress of the eclipse, the two groups are fully resolved. In such cases additional change of the centroid caused by the proper motion or parallax effect are hard to be distinguished from other factors. That is why we examined these stars separately in greater details

(see Section 6.5). Stars within  $1''$  radius from each variable were removed, which resulted in decreasing the sky area surveyed by 0.036 and 0.006 square degrees for the LMC and the SMC, respectively. The list of variable stars was taken from the on-going research on the OGLE-III Catalog of Variable Stars (hereinafter OIII-CVS) which includes classical, type II and anomalous Cepheids, RR Lyr variables, long period variables,  $\delta$  Sct stars, R CrB variables, eclipsing binary systems and the so-called double periodic variables (last four types of variable stars are from the LMC fields only). OIII-CVS was presented in a series of papers (*e.g.*, Soszyński *et al.* 2009ab, Graczyk *et al.* 2011).

Additional candidate variable stars can be selected using the dispersion of photometric measurements. We did not do this because in the DIA photometry significant changes of the measured flux can be caused by the motion of the star (Eyer and Woźniak 2001). When the distance between current position of the star and its position on the reference image is comparable to the diameter of the circle in which the stellar flux is estimated, the measured flux is smaller than the actual value. Because of the changing distance between the star and its position on the reference image, the magnitudes measured using DIA appear to be linear function of time or quadratic function of time. In this last case the vertex of the parabola corresponds to the epoch when the actual and reference positions of the star coincided. For such light-curves the dispersion of photometric measurements can be significant which hampers clear separation of variable stars from the ones with high proper motions.

The results of fitting the model to the data using the least-squares method may be significantly changed by outlying measurements, even if their number is relatively small. In most cases one removes such points using *e.g.*,  $3\sigma$  criterion and fits the model once more. It is not obvious how one can remove outlying points and do not change the derived  $\mu$  and  $\pi$  for astrophysically important objects (*e.g.*, close CPM binaries) at the same time. Thus, instead of removing outlying points we decided to select stars with reliably derived proper motions and publish only them.

For selected stars with the proper motions higher than 20 mas/yr we examined plots of centroids positions in  $(\alpha(t), \delta(t))$  plane with color-coded epoch of the observation  $t$ . Fig. 1 presents example plot showing not moving object (left) and a star with significant proper motion (right). For stars with the proper motions higher than the chosen limit, in most cases one easily recognizes that either the star is moving or the proper motion derived is caused by blending with nearby object, small number of epochs, large scatter of data-points etc. Fig. 2 presents the diagram of the  $\chi^2$  (reduced) of the model fitted *vs.*  $I$ -band brightness for a sample of stars. Gray circles mark the stars which passed the visual examination, while black crosses the ones that failed. Based on a clear division between the two groups we defined the region on the graph which gave high reliability of the proper motions. The division is shown by black line in Fig. 2 and we call it the  $\chi_{\text{lim}}^2(I)$  criterion. Even though this region was derived using stars with  $\mu > 20$  mas/yr, it was used to automatically select stars with well fitted parameters among the whole sample

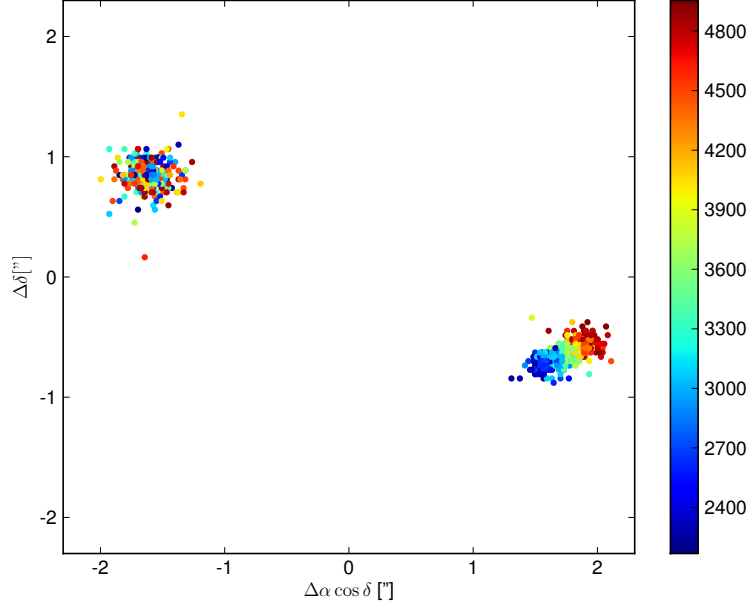


Fig. 1. Example plot of positions in R.A. and Dec. direction with color-coded epoch of observation. The bar shows the color scale of the epoch of observation  $HJD - 2450000$ . The star on the right-hand side has significant proper motion and the one on the left-hand side is not moving (*i.e.*, belongs to MCs).

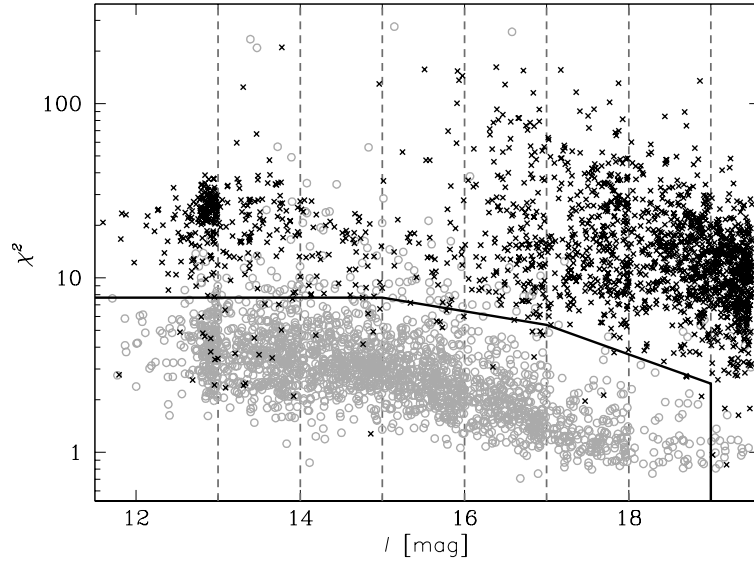


Fig. 2.  $\chi^2$  of Eqs.(1) and (2) model fitting vs.  $I$ -band brightness diagram for a subset of stars visually verified. In each 1 mag range (marked by dashed vertical lines) 500 stars were selected randomly among objects with  $\mu > 20$  mas/yr. The gray circles correspond to the stars which passed the verification and the black crosses – to the ones which failed. Black line marks the region which is used for automated selection of stars with reliable proper motion.

of stars. Table 1 presents, in seven brightness ranges, reliability of this criterion *i.e.*, the number of stars with confirmed proper motions divided by the number of all stars within the selected area. In almost all cases it turned out to be higher than 95%. Table 1 also presents the completeness which is understood as the ratio of the number of stars with confirmed proper motions which fulfill the  $\chi_{\text{lim}}^2(I)$  criterion to the number of all stars for which proper motions could be measured reliably using our data set.

Table 1

Statistical properties of criterion applied

magnitude range	reliability	completeness
< 13 mag	95.1%	93.9%
13 – 14 mag	96.9%	92.6%
14 – 15 mag	97.7%	93.2%
15 – 16 mag	98.9%	93.6%
16 – 17 mag	98.1%	95.1%
17 – 18 mag	98.2%	98.2%
18 – 19 mag	93.9%	92.0%

For the stars fainter than  $I = 19$  mag the scatter of the individual centroids is so large that examination of our plots did not give firm conclusions on the proper motion reliability. Thus, we removed all stars fainter than 19 mag. The stars which did not pass the  $\chi_{\text{lim}}^2(I)$  criterion were checked, if the fit performed using only centroids from the images with seeing better than arbitrarily chosen limit of  $1''.17$  gave  $\chi^2$  below the limit. This way the number of stars fulfilling our criteria raised by 2.3%.

The visual examination was performed not only to derive the region on  $\chi^2$  vs.  $I$  plane which corresponded to the well fitted stars. We also examined the stars of particular interest *i.e.*, the ones with the proper motions higher than 70 mas/yr (no matter whether fulfilling the  $\chi_{\text{lim}}^2(I)$  criterion or not), the parallax higher than 15 mas, candidate WDs and candidate members of CPM binaries with  $\mu > 30$  mas/yr. We note that in this step the reliability of the proper motion was checked, but not the parallax. All the stars that passed the visual examination were included in the catalog, even if they did not fulfill the  $\chi_{\text{lim}}^2(I)$  criterion. The stars which fulfilled this criterion and did not pass the visual examination were not included to the final catalog.

The parallaxes were estimated for all the stars. If the number of observations for a given star was small, fitting the model with a smaller number of parameters should be preferred. Thus, the parallaxes are given only if the number of measurements was higher than 200 for objects in the LMC fields and 300 for objects in the SMC fields. The limit was set higher for the SMC fields, because the distribution of epochs in these fields hampers parallax estimation. The obvious requirement

was that the normal matrix in the fitting procedure was not ill conditioned. To allow statistical modeling of the Galaxy kinematics, contrary to Paper I, we did not put any lower limit on the significance of given parallaxes including even negative parallaxes.

For simplicity, the coordinates given in the catalog are the same as ones given by Udalski *et al.* (2008bc or Paper I). We note here that the epochs to which reference images correspond are between 2001.9 and 2006.9 and can be found in the headers of the FITS files published by Udalski *et al.* (2008bc). The differences between the J2000.0 epoch position and the ones given by Udalski *et al.* (2008bc) are in the range  $0''.6$ – $0''.7$  for only 25 objects presented. The differences are between  $0''.5$  and  $0''.6$  for less than 220 stars and for the rest of the stars the differences are smaller. The OGLE-III fields were overlapping and in some cases two, three or even four records are given in the catalog for one star. We encourage the catalog users to apply their own selection criteria.

#### 4. Data Access

The catalog of proper motions for stars observed by the OGLE-III survey in the direction of the MCs is available for the astronomical community only in the electronic form *via* FTP site:

*ftp://ftp.astrouw.edu.pl/ogle/ogle3/pm/mcs/*

The catalog is divided into 1256 files, one for each of the OGLE-III subfields. For each star we provide: the OGLE-III identifier, J2000.0 equinox coordinates as well as *I*-band brightness and (*V* – *I*) color (all taken from Udalski *et al.* 2008bc or Paper I), proper motion per coordinate in both directions ( $\mu_{\alpha^*} = \mu_{\alpha} \cos \delta$  and  $\mu_{\delta}$ ) with statistical and systematic uncertainties given separately (six fields altogether), total proper motion  $\mu = \sqrt{\mu_{\alpha^*}^2 + \mu_{\delta}^2}$ , parallax and its uncertainty if available, differential refraction coefficient and its uncertainty,  $\chi^2$  per degree of freedom for the model used,  $\chi_{\text{lim}}^2(I)$  value, number of data points used for fitting and flags showing objects which were visually verified and ones for which only data from the best seeing images were used. The units of proper motions are milliarcsecond per year (mas/yr). Both the parallaxes and the differential refraction coefficients are given in mas. Stars presented in Paper I are added for consistency.

Together with the main catalog the files *CPM.dat* and *variables.dat* are distributed. The first of them describes the CPM systems found (Section 6.2) and the second one gives the proper motions of the variable stars (Section 6.5). Remarks to specific objects are given in *remarks.txt* file. The detailed description of all the catalog files is given in the *README* file.



## 5. Catalog Properties

We note that small number of objects in the catalog (1.6% of the sample) does not have  $V$ -band magnitude. For these objects and in the field SMC140 covering central part of 47 Tuc our results are less certain.

### 5.1. Completeness

The completeness of our catalog depends on the proper motion value. For stars published in Paper I, *i.e.*, the ones with  $\mu \geq 100$  mas/yr, a very detailed selection procedure was applied, including case-by-case study of the time series astrometry. In Paper I we compared our list with other published catalogs (Alcock *et al.* 2001, Soszyński *et al.* 2002) showing its very high completeness. The completeness is only slightly worse for stars with  $70 \text{ mas/yr} \leq \mu < 100 \text{ mas/yr}$ , as all the stars with the proper motions in this range were visually verified, even if they did not pass the  $\chi_{\text{lim}}^2(I)$  criterion. All the stars with  $30 \text{ mas/yr} \leq \mu < 70 \text{ mas/yr}$  passing the  $\chi_{\text{lim}}^2(I)$  criterion were also visually verified. To find this criterion, we inspected also randomly chosen stars with  $20 \text{ mas/yr} \leq \mu < 70 \text{ mas/yr}$ , which made their list more reliable and complete than the list of stars with  $\mu < 20 \text{ mas/yr}$ .

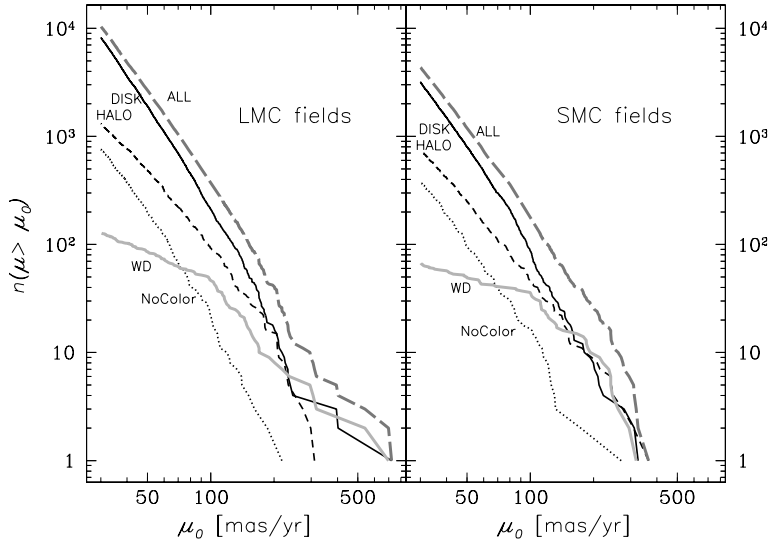


Fig. 3. Number of objects with proper motions higher than the given limit  $\mu_0$  for all objects (dashed dark gray line) and separately for: disk stars (black solid line), halo stars (dashed line), WDs (light gray line) and the stars without color information (dotted line). *Left panel* presents results for the LMC fields, while right one – for the SMC fields.

It was checked how the number of stars with  $\mu > 30$  mas/yr assigned as disk dwarfs, halo dwarfs, WDs and stars without color information (see Section 6.1) depends on  $\mu$ . It is shown in Fig. 3. Only for WD group the dependence breaks at  $\mu \approx 100$  mas/yr. We did not find good explanation for it. In the range  $35 \text{ mas/yr} <$

$\mu_0 < 100$  mas/yr we fitted following relations to the cumulative distribution of all stars (the LMC and the SMC fields separately):

$$\log_{10} n_{\text{LMCf}}(\mu > \mu_0) = -2.80 \log_{10} \mu_0 + 8.16 \quad (3)$$

$$\log_{10} n_{\text{SMCf}}(\mu > \mu_0) = -2.68 \log_{10} \mu_0 + 7.62 \quad (4)$$

These cumulative distributions were used (see Section 6.2) to statistically quantify whether the pairs of stars located close to each other on the sky are highly probable CPM systems or only chance alignments.

The total number of foreground Galactic stars can be estimated by counting stars with significance of proper motions higher than  $5\sigma$ . Out of our 6.2 million stars 440 000 objects satisfy this criterion.

### 5.2. Accuracy of the Proper Motions and Parallaxes

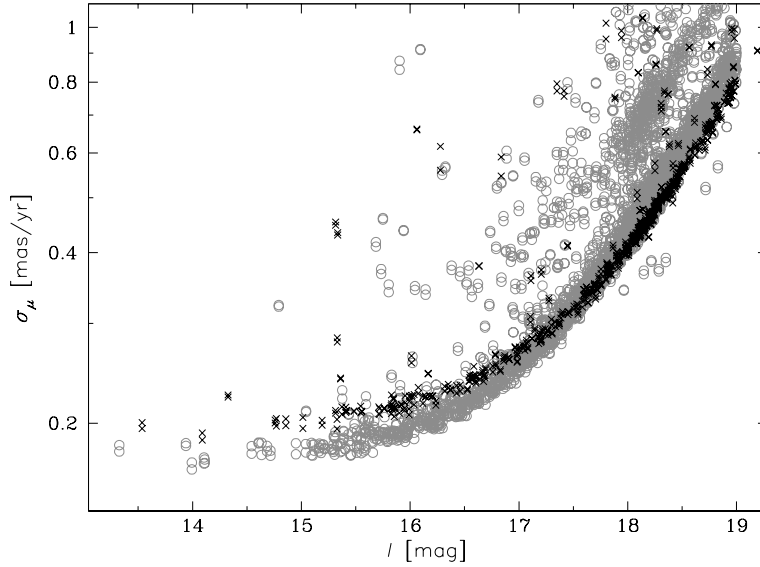


Fig. 4. Proper motion uncertainties as a function of brightness. The crosses correspond to the stars located in a sparse subfield LMC152.1, while gray circles – in a dense subfield LMC161.1. Outlying points with  $\sigma_\mu > 1.1$  mas/yr are not shown. They compromise around 3% of the stars in each field. In the LMC161.1 subfield a group of stars fainter than 18 mag with the uncertainties larger by  $\approx 30\%$  than most of the stars with similar brightness is composed of the stars which passed the selection criterion after removing centroids from images with seeing worse than  $1''.17$ . Two points are given for each star depicting uncertainties in R.A. and Dec. directions separately.

Fig. 4 presents the formal uncertainties of the proper motions for stars in a dense and a sparse stellar fields with similar number of epochs. In the dense field the uncertainties for the brightest stars are smaller than in the sparse one because of the higher number of stars used in the frames' alignment. For stars brighter than 18.5 mag the uncertainties are smaller than 0.5 mas/yr.

As it was presented in Paper I the uncertainties of the parallaxes are down to 1.6 mas. The possible effects which may cause systematic offsets in the parallaxes are too simple description of the differential refraction and non-zero parallaxes of stars used to calculate corrections of positions. To calculate these corrections we used stars with  $\mu < 20$  mas/yr (Paper I) but even these stars may influence the zero point of parallaxes comparably to the smallest uncertainties.

## 6. Discussion

### 6.1. Physical Properties

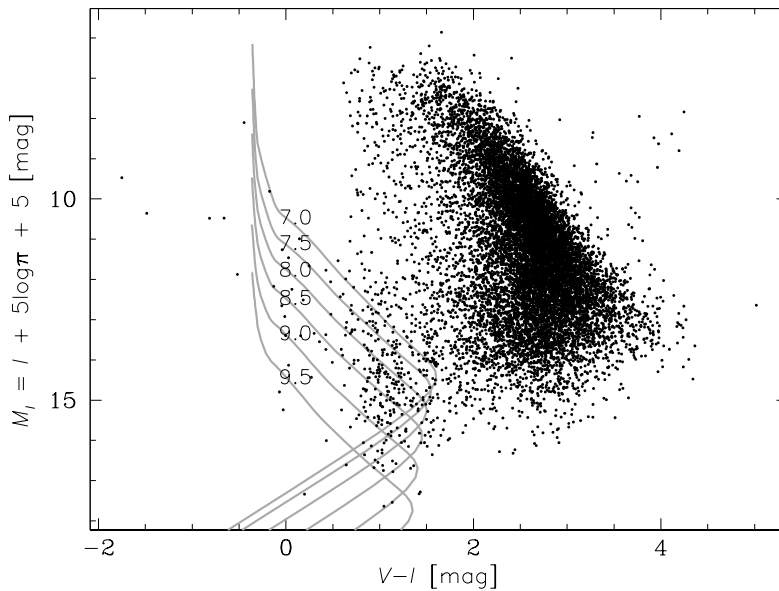


Fig. 5. Hertzsprung-Russell diagram based on geometric parallaxes. Only stars with  $\pi/\sigma_\pi > 3$  are shown. Error bars are not shown for clarity. Gray lines present theoretical models for pure Hydrogen WDs by Holberg and Bergeron (2006) with  $\log g$  values given next to each line.

The Hertzsprung-Russell diagram for stars with  $\pi/\sigma_\pi > 3$  is presented in Fig. 5. The main sequence (MS) is clearly visible. Theoretical WD positions are plotted based on Holberg and Bergeron (2006) models. In total, there are  $\approx 270$  WDs in the part of the diagram enveloped by the theoretical models. Subdwarfs, which are 2–4 mag fainter than the MS can also be selected.

The other way, one can verify luminosity class and additionally find population to which the stars belong, is to plot the reduced proper motion (hereafter RPM, defined as  $H_I = I + 5 \log \mu$ ) as a function of the  $(V - I)$  color. If all the stars had the same tangential velocities, it would be the same as H–R diagram shifted vertically by the value depending on the velocity. Fig. 6 shows the RPM for objects with  $\mu > 30$  mas/yr. Lines separating WDs from halo dwarfs (dashed line) and

halo dwarfs from disk dwarfs (dotted line) were determined to give the best discrimination of different stellar populations. Based on these lines each object was labeled as WD, halo dwarf, disk dwarf or star without  $(V - I)$  color information. The distribution of stars in our RPM diagram is similar to the ones derived by other authors (*e.g.*, Chanamé and Gould 2004, Sesar *et al.* 2008).

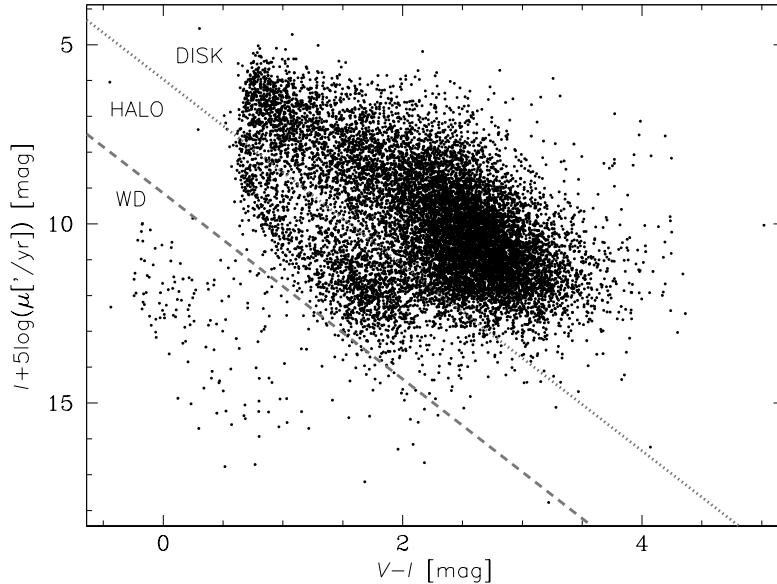


Fig. 6. Reduced proper motion diagram for all stars with  $\mu > 30$  mas/yr. Dashed line separates WDs from halo stars while dotted line separates halo stars from disk stars.

## 6.2. Common Proper Motion Systems

To search for the CPM binaries we used the stars with  $\mu > \mu_{\text{lim}} = 30$  mas/yr. The edges of the OGLE-III fields were overlapping, thus, before the search was started a list of unique stars with  $\mu > \mu_{\text{lim}}$  was prepared. It contained 10 405 stars located in the LMC fields and 4378 stars located in the SMC fields. All of them were inspected visually, not only to check the reliability of the results, but also to find the CPM companions at the separations around  $1''$ . In such close systems the mean magnitudes of components may be inaccurately measured. For some stars we manually removed outlying points and fitted the model once more.

All the stars were searched for companions closer than  $1500''$ . Each pair was verified similarly to Chanamé and Gould (2004). First, by comparing the angular distance of the components ( $\Delta\theta$ ) and the vector proper motion difference ( $\Delta\mu$ ) with a distribution of unrelated pairs. These distributions were normalized based on the number of stars with proper motions higher than the proper motion of the pair. We report all the CPM binaries which passed this selection. Second, it was checked on the RPM diagram if both components belong to the same population. We describe these two steps below and present the most interesting systems.

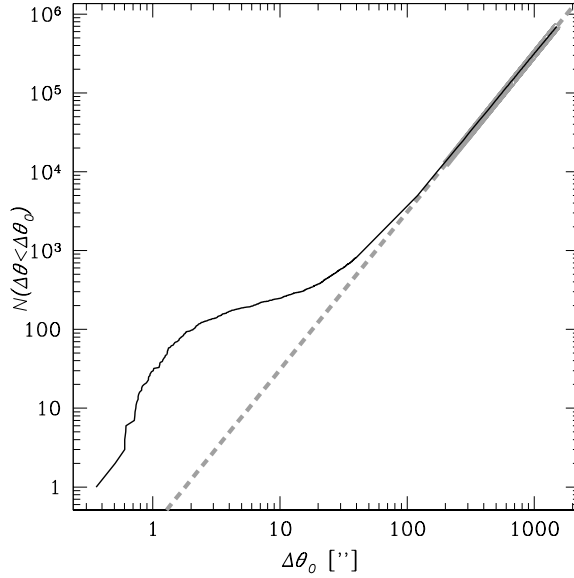


Fig. 7. Cumulative distribution of number of pairs as a function of angular separation for all pairs of stars with  $\mu > 30$  mas/yr in the LMC fields with  $\Delta\theta < 1500''$ . The gray line shows the relation for unrelated pairs. Thick part corresponds to the region where the fit was performed and dashed part is an extrapolation.

The expected number of unrelated pairs ( $N_{UP}$ ) with angular separations greater than the value for a given pair ( $\Delta\theta_0$ ), the vector proper motion difference ( $\Delta\mu$ ) smaller than the value for a given pair ( $\Delta\mu_0$ ), and which are found among stars with proper motions larger than for a given pair ( $\mu_0$ ), was estimated based on:

$$N_{UP}(\Delta\theta_0, \Delta\mu_0, n(\mu > \mu_0)) = N(\Delta\theta < \Delta\theta_0, n(\mu > \mu_0))p(\Delta\mu < \Delta\mu_0) \quad (5)$$

where  $n(\mu > \mu_0)$  is the number of stars with proper motion larger than  $\mu_0$  in the LMC fields (Eq. 3) or in the SMC fields (Eq. 4),  $N(\Delta\theta < \Delta\theta_0, n)$  denotes the number of unrelated pairs with separations smaller than  $\Delta\theta_0$  found among  $n$  stars, and  $p(\Delta\mu < \Delta\mu_0)$  is the probability that an unrelated pair has the proper motion vector difference ( $\Delta\mu$ ) smaller than  $\Delta\mu_0$ .

Fig. 7 presents the cumulative number of pairs (black line) as a function of  $\Delta\theta$  based on all pairs with separations  $\Delta\theta < 1500''$  found among 10 405 stars in the LMC fields. Genuine CPM binaries are expected to have small values of  $\Delta\theta$ , and the excess of binaries with  $\Delta\theta \lesssim 20''$  is evident. It is expected that the number of unrelated pairs increases as a square of  $\Delta\theta_0$ . Very small number of pairs with  $\Delta\theta$  in the range between  $200''$  and  $1500''$  are expected to be CPM binaries. The total of over 680 000 pairs found in this range results in the fit

$$N(\Delta\theta < \Delta\theta_0) = 0.31 \Delta\theta_0^2$$

The gray line in Fig. 7 presents this relation. The slope of observational data is very close to the expected one in the range of  $\Delta\theta$  where the fit was found. From this fit

we found that the separation within which one unrelated pair is expected is as small as  $1.''8$ .

The number of unrelated binaries scales also as a square of the number of stars used for search ( $n$ ). The above search was performed with  $n = 10405$ . This allows to rewrite the above equation for  $N$  taking into account  $n$ :

$$N(\Delta\theta < \Delta\theta_0, n) = 2.9 \cdot 10^{-9} n^2 \Delta\theta_0^2 \quad (6)$$

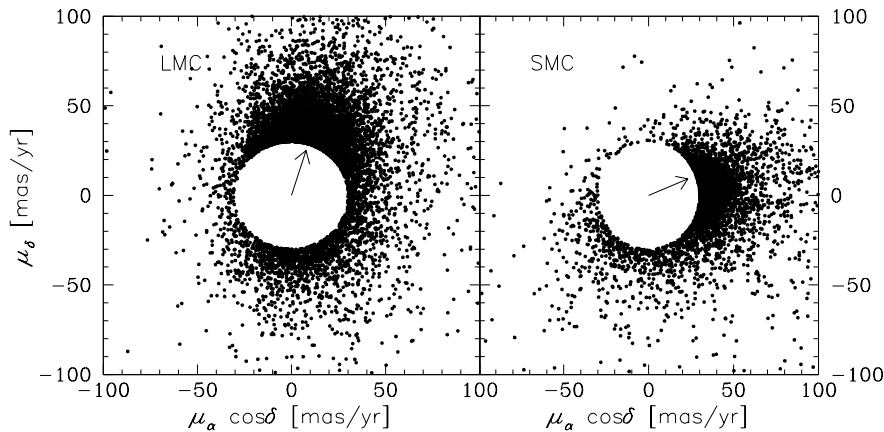


Fig. 8. Proper motion vector-point diagram for stars in the LMC fields (*left panel*) and the SMC fields (*right panel*). Only stars with  $\mu > \mu_{\text{lim}}$  are shown. The figures are limited to the absolute values of proper motions per coordinate below 100 mas/yr. The arrows indicate the average direction of the solar anti-apex based on Schönrich *et al.* (2010). The position angle of solar anti-apex direction for individual star may deviate from the average up to  $18.^{\circ}5$  in the LMC fields and up to  $9.^{\circ}5$  in the SMC fields.

To estimate  $p(\Delta\mu < \Delta\mu_0)$  probability one can assume that  $\mu_{\alpha\star}$  and  $\mu_{\delta}$  are random variables taken from a distribution with known properties. In such a case the formula for  $p(\Delta\mu < \Delta\mu_0)$  could be found based on theoretical basis with the parameter fitting as we did for  $N(\Delta\theta < \Delta\theta_0, n)$ . Fig. 8 presents the proper motion vector-point diagram for stars with  $\mu > 30$  mas/yr and located in the LMC fields (*left panel*) and the SMC fields (*right panel*). Even without the  $\mu_{\text{lim}}$  limit these distributions could not be well approximated by bivariate Gaussian distributions. That is because the vectors of solar anti-apex are not the axes of reflection symmetry of these distributions. Proper description of such distributions using distributions with known properties would be very challenging task. Thus, to estimate  $p(\Delta\mu < \Delta\mu_0)$  we used the cumulative distribution functions (CDFs) of  $\Delta\mu$  for pairs with  $\Delta\theta > 200''$ . As it was mentioned before, almost all of these pairs are expected to be unrelated. Solid line in Fig. 9 shows the CDF of  $\Delta\mu$  for the pairs in the LMC fields with  $\Delta\theta > 200''$ . For comparison we plot on the same figure CDF of  $\Delta\mu$  for pairs with  $\Delta\theta < 7''$  (dashed line) which are mostly expected to be CPM binaries. The much faster increase of the dashed line compared to the solid line, proofs that

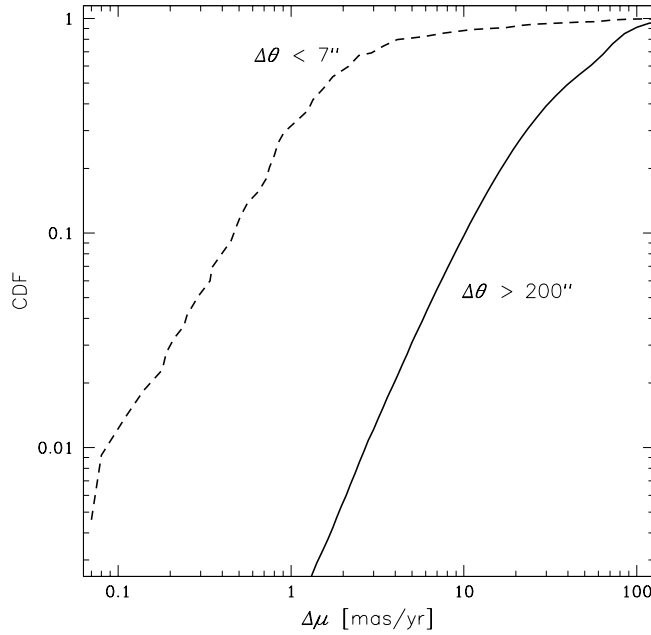


Fig. 9. Cumulative Distribution Functions (CDF) of  $\Delta\mu$  for the pairs in the LMC fields with separations  $\Delta\theta > 200''$  (i.e., unrelated pairs; solid line) and  $\Delta\theta < 7''$  (i.e., mostly CPM binaries; dashed line).

closer pairs have components of similar proper motion. The CDF of pairs with  $\Delta\theta > 200''$  in the SMC fields overlays the one for the LMC fields and is not plotted for clarity.

For each pair fulfilling the criteria  $\Delta\theta < 1500''$  and  $\Delta\mu < 30$  mas/yr, we calculated  $N_{UP}(\Delta\theta_0, \Delta\mu_0, n(\mu > \mu_0))$ . The  $n(\mu > \mu_0)$  parameter was estimated based on Eqs. (3) or (4) for the LMC and the SMC fields, respectively. Eq. (6) was used to calculate  $N(\Delta\theta < \Delta\theta, n)$  and  $p(\Delta\mu < \Delta\mu_0)$  probability was empirically found based on the CDF of  $\Delta\mu$  (Fig. 9). Most of the CPM binaries should have small values of  $N_{UP}$ . We decided to search for pairs with  $N_{UP}(\Delta\theta_0, \Delta\mu_0, n(\mu > \mu_0)) < 0.75$ , which resulted in 316 pairs in the LMC fields and 214 pairs in the SMC fields. All of them are reported in the file *CPM.dat*. The sum of  $N_{UP}(\Delta\theta < \Delta\theta_0, \Delta\mu < \Delta\mu_0, n(\mu > \mu_0))$  values for all reported pairs resulted in 53.8, which is the expected number of unrelated pairs in the selected sample.

Next, we verified whether for pairs composed of halo or disk stars their components have positions on the RPM diagram consistent with the positions expected for coeval objects belonging to the same population. As noted by Chanamé and Gould (2004) the components of CPM binary should lie on the line parallel to the MS track. Each pair was flagged as either consistent, inconsistent or questionable. There are 70 pairs containing WDs or stars without color information, which are not characterized in this way. Also for 98 pairs containing stars located very close

to each other on the sky or on the RPM diagram verification is not possible. For verified objects there were 256 (71%) marked as consistent, 71 (20%) as inconsistent and 35 (9.7%) as questionable.

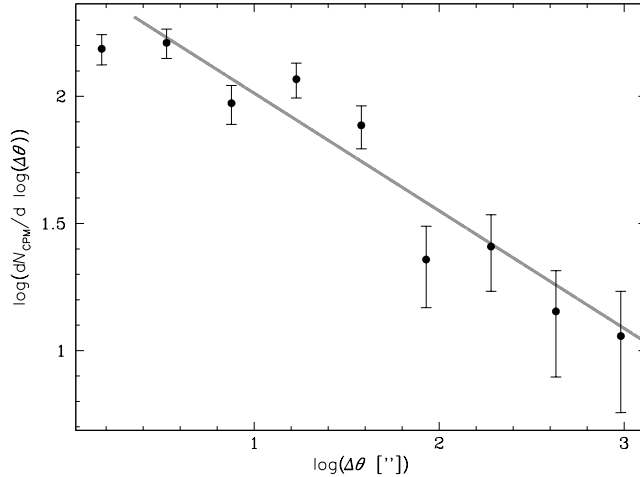


Fig. 10. Distribution of disk CPM binaries angular separations. The error bars were calculated assuming Poisson statistics.

Fig. 10 presents the distribution of the disk CPM binaries (confirmed using the RPM diagram) as a function of angular separation. All the points except the one for the smallest  $\Delta\theta$  were used to make a linear fit (gray line). If we assume that the number of CPM ( $N_{\text{CPM}}$ ) scales as  $N_{\text{CPM}} \approx \theta^{-\alpha}$  then the inclination of the best-fitting line gives the estimated power-law exponent  $\alpha$  of  $1.46 \pm 0.02$ . This value is significantly smaller than the  $1.67 \pm 0.07$  value found by Chanamé and Gould (2004). We suspect this discrepancy is caused by the stellar streams which we observe in the narrow solid angle analyzed here. The impact of stellar streams is reduced in the whole sky analysis such as the one by Chanamé and Gould (2004). The median parallax of the CPM binaries used in a fit is 4.4 mas which translates to the typical distance almost four times larger than in Chanamé and Gould (2004) sample. Only the first point in Fig. 10 deviates significantly from the linear fit, thus, the completeness of our sample of CPM binaries seems constant in the range from  $2''$  to  $\approx 1000''$ . The number of confirmed halo CPM binaries is too small to perform an analysis of the angular separations' histogram.

One candidate pair containing a WD and a halo star *i.e.*, LMC155.1.4867 and LMC155.1.5999 was announced in Paper I. Monteiro *et al.* (2006) observed a similar pair to estimate the age of the red subdwarf. Similar research can be done using LMC155.1.4867-LMC155.1.5999 pair, in which additionally the distance of both components is larger, brightness difference is smaller, and brighter component does not affect observed spectrum of the fainter component, as was a case for Monteiro *et al.* (2006) observations. Other interesting pair from Paper I con-



tains two WDs (LMC102.7.22769 and LMC102.7.22886). The separation of these objects is  $92''$ . There are only 32 other WD-WD CPM systems known (Sion *et al.* 1991, Jordan *et al.* 1998, Scholz *et al.* 2002, Farihi *et al.* 2005 and reference therein). The LMC107.2.14205-LMC107.3.195 pair with  $\Delta\theta = 593''$  was confirmed on the RPM diagram. If parallaxes of the components ( $9.2 \pm 1.6$  mas and  $9.4 \pm 1.6$  mas, respectively) are taken into account, this angular separation translates into the projected physical separation of 0.31 pc, which is the largest value among the RPM-confirmed systems presented here and with significant parallaxes of both components.

It is possible to search and verify in detail CPM binaries among stars with lower proper motion limit. The number of candidate CPM binaries, selected based on the expected number of unrelated pairs, scales as  $\mu_{\text{lim}}^{-2.5}$ . For a search performed on the list of stars with  $\mu_{\text{lim}} = 20$  mas/yr, we can expect a total of around 1460 candidate CPM binaries. The preparation of the reliable list of such binaries requires much of additional effort and is beyond the scope of this paper.

### 6.3. Relative Proper Motion of 47 Tuc and SMC

The relative proper motion of the Galactic globular cluster 47 Tuc and SMC was measured in the two subframes of the SMC136 field and averaged. These subframes contained a reasonably high number of bright stars ( $I < 17.7$  mag) belonging to both environments – 112 in the SMC and 113 in 47 Tuc. Table 2 lists the literature values of the relative proper motion and includes our estimate. The measurements of absolute proper motion of 47 Tuc were transformed to relative values based on the absolute proper motion of the SMC from Piatek *et al.* (2008) *i.e.*,  $\mu_{\text{SMC},\alpha^*} = 0.754 \pm 0.061$  mas/yr and  $\mu_{\text{SMC},\delta} = -1.252 \pm 0.058$  mas/yr. The only measurement which is significantly more accurate than ours is based on the Hubble Space Telescope (HST) observations (Anderson and King 2003).

Table 2

Relative proper motions of 47 Tuc and SMC

Source	$\mu_{\alpha^*}$ [mas/yr]	$\mu_{\delta}$ [mas/yr]
Tucholke (1992)	$5.5 \pm 2.0$	$-1.6 \pm 2.0$
Odenkirchen <i>et al.</i> (1997) <sup>a</sup>	$6.2 \pm 1.0$	$-4.05 \pm 1.0$
Freire <i>et al.</i> (2001) <sup>a</sup>	$5.8 \pm 1.9$	$-2.15 \pm 0.6$
Freire <i>et al.</i> (2003) <sup>a</sup>	$4.5 \pm 0.6$	$-2.05 \pm 0.6$
Anderson and King (2003)	$4.716 \pm 0.035$	$-1.357 \pm 0.021$
Girard <i>et al.</i> (2011) <sup>ab</sup>	$6.9 \pm 1.0$	$-2.1 \pm 1.0$
this work	$4.41 \pm 0.67$	$-1.12 \pm 0.55$

<sup>a</sup> – shifted based on the absolute proper motion of the SMC by Piatek *et al.* (2008); <sup>b</sup> – uncertainty anticipated by the authors is given;

#### 6.4. *Absolute Proper Motion of the Magellanic Clouds*

There are 200 quasars known behind the LMC (Kozłowski *et al.* 2012). Most of the brightest ones are close to stars of similar brightness which hampers the determination of the proper motion with the highest possible accuracy. Our data do not permit the determination of the proper motion of the LMC or the SMC against quasars with accuracy comparable to the HST one (Piatek *et al.* 2008).

#### 6.5. *Proper Motions of Variable Stars*

Proper motions of variable stars for which absolute magnitudes can be estimated using other methods (*e.g.*, RR Lyr variables) can be used to analyze statistical properties of their kinematics and distribution (*e.g.*, Martin and Morrison 1998, Kinman *et al.* 2007). To allow similar analysis, we separately present proper motions for stars from OIII-CVS.

As discussed earlier, measuring the proper motion of a variable star is more complicated than for a constant star. All the variable stars for which at least one model resulted in a significant proper motion were visually inspected similarly to the method shown in Fig. 1. We paid special attention to check, if for these stars the observed motion was not caused by the light variations on a very long time-scales. In such cases the apparent motion might be a result of blending only. No significant parallaxes for the variable stars were found.

There are three possible astrophysical situations in which the proper motion of a variable star observed toward the MCs may be significant: (i) a variable star is located in the foreground of the MCs, (ii) a variable star in the MCs is blended with a foreground object, which causes the centroid of both objects to move and (iii) variable star in the MCs has an exceptionally high tangential velocity and it is possibly a runaway object. For some of the low signal-to-noise variables (*e.g.*,  $\delta$  Sct pulsators and smallest amplitude long period variables) it is possible that the claimed variability is caused by the photometric noise. The situation (i) can in most cases be verified based on the position of the object in the color–magnitude diagram (CMD) or the period–luminosity diagram. The situation (ii) can be verified using high spatial resolution imaging. The last possibility is quite unlikely and if confirmed, would reveal very rare objects.

A group of variable stars to which we pay special attention were blue variables from LMC. Sabogal *et al.* (2005) claimed that in the LMC these stars separate into two groups in the CMD. One group contains stars redder than  $(B - V) = 0.4$  mag. Most of those stars have  $-0.3 \text{ mag} < (B - V) < 0.0 \text{ mag}$ . The second group, which has not been seen in the SMC, contains stars with the colors in the range of  $0.4 \text{ mag} < (B - V) < 0.6 \text{ mag}$ . We have cross-matched these stars with our catalog of proper motions and it turned out that the stars from the second group are not blue variables from the LMC but Galactic stars which are observed in the direction of the LMC. In the second group 87.5% of stars had proper motions larger than 4 mas/yr, while in the first one this number was only 0.5%. Most probably the

brightness changes seen in the photometry were caused only by the change of the stellar centroids (Alcock *et al.* 2001, Eyer and Woźniak 2001). Our finding is confirmed by the color-color diagram shown by Sabogal *et al.* (2005) in which the stars from the second group follow main sequence track of spectral types later than F5.

The variable stars with significant proper motions are presented in a separate file *variables.dat*. It contains OIII-CVS identifier, equatorial coordinates and proper motions ( $\mu_{\alpha^*}$ ,  $\mu_{\delta}$  and  $\mu$ ). In total 236 variable stars are presented. Most of them (162) are eclipsing binaries. Three CPM binaries containing variable stars are indicated in *remarks.txt* file distributed with the catalog.

### 6.6. Cepheid Instability Strip

The catalog of proper motions can be used to check if a given set of stars belong to the MCs or the Galaxy. Below, we present one of possible applications – a search for non-variable stars in the LMC which are located in the part of the CMD populated by the classical Cepheids (Soszyński *et al.* 2008). Foreground stars are major contaminants in this part of the diagram and we removed them using proper motions, which is described below.

The left panel of Fig. 11 presents the mean *I*-band brightness vs. *I*-band amplitude for fundamental mode Cepheids in the LMC. The right panel of Fig. 11 shows the CMD of these Cepheids. As we wanted to restrict our search to the region of CMD where Cepheids are efficiently found and high accuracy proper motions are available, we limited brightness range to  $13.5 \text{ mag} < I < 15.5 \text{ mag}$  (shown on both panels of Fig. 11) and used objects lying between two inclined lines on the CMD (shown on the right panel of Fig. 11). These four lines constrain the part of the CMD from which stars are further analyzed. Except the Cepheids there are 14 840 stars in our selection region for which the proper motions were obtained from the catalog. In order to remove Galactic objects from the sample we selected stars with proper motions consistent with the LMC ones ( $\mu < 2 \text{ mas/yr}$ ) and consistent with zero within  $2\sigma$  limit. In total 1361 stars fulfilled all the above constraints. Their positions are shown in Fig. 12 with the LMC image from the ASAS survey in the background. The selected objects clearly clump in the bar of the LMC, which is another strong suggestion that most of them belong to that galaxy.

The blending scenario can be verified for some of these objects using the existing HST observations. Ground-based Strömgen photometry of these objects was already obtained in selected fields. When analyzed it will give the final verification if these objects are dwarfs or white dwarfs and thus belong to the Galaxy, or are giants and supergiants and thus belong to the LMC. The latter case will allow observational mapping of the Cepheid instability strip.

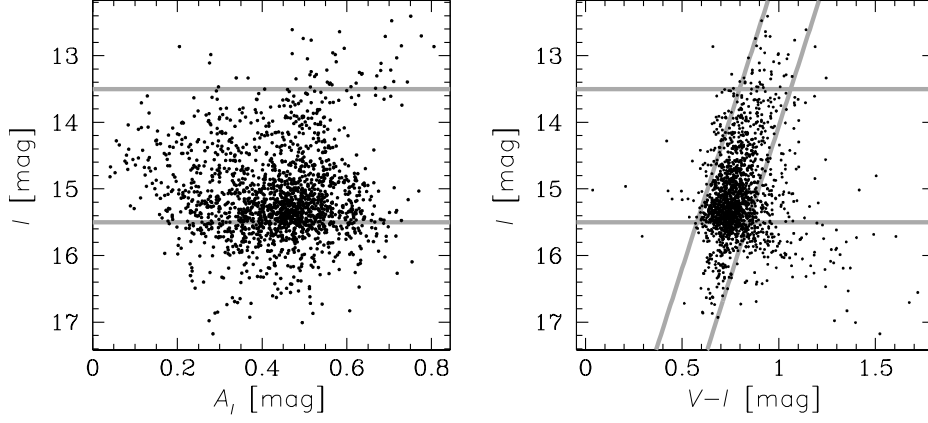


Fig. 11. *Left panel*:  $I$ -band brightness vs.  $I$ -band amplitude for fundamental mode Cepheids in the LMC. *Right panel*: CMD of those Cepheids. Gray lines constrain the part of the CMD from which constant stars are further analyzed.

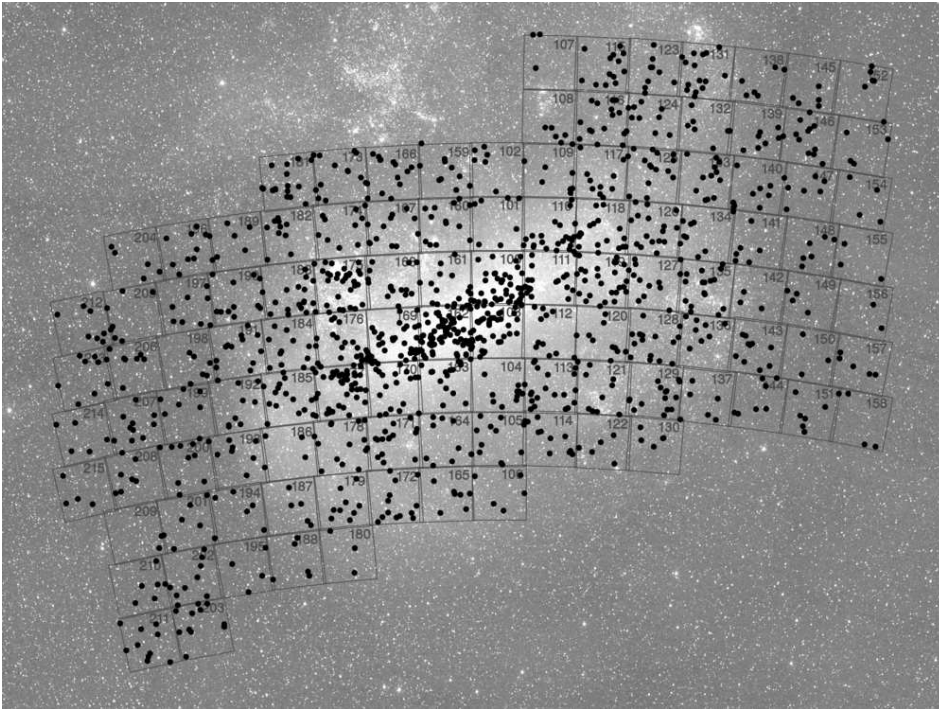


Fig. 12. Sky projection of constant objects with proper motions consistent with the LMC and located inside the region defined in the right panel of Fig. 11. Background image comes from the ASAS survey (Pojmański 1997). The squares represent the OGLE-III fields with field number given for each of them.

## 7. Summary

The presented catalog gives proper motions for stars observed in the directions of the LMC and the SMC. For bright stars the accuracy is below 1 mas/yr including systematic uncertainties. Uncertainties of the derived parallaxes are down to 1.6 mas.

Beside presenting the catalog itself, we outlined a few ways it can be used. Geometrically measured parallaxes were used to construct the Hertzsprung-Russell diagram, which permits the selection of  $\approx 270$  WDs. The RPM diagram enabled the discrimination of the stars belonging to the Milky Way halo from disk objects. Among the stars with the proper motion  $\mu > 30$  mas/yr we searched for the CPM binary systems. Based on statistical considerations more than 500 candidate CPM binaries were selected. Among pairs which could be verified on the RPM diagram 7.7% showed positions inconsistent with any isochrone. The distribution of the RPM-confirmed disk CPM binaries is well fitted with a power law exponent of  $1.46 \pm 0.02$ , which is significantly smaller than the  $1.67 \pm 0.07$  value found by Chanamé and Gould (2004). Among CPM binaries one candidate for a WD-WD pair and one candidate for a halo star-WD were found. In order to assess the accuracy of our measurements, we determined the proper motion of 47 Tuc globular cluster and compared it with other estimates. Measurements significantly better than ours were obtained only using the HST. We payed special attention to the variable stars for which proper motions were presented separately. The existence of blue LMC variables with  $(B - V) > 0.4$  mag, claimed by Sabogal *et al.* (2005), was neglected.

The catalog may be used to prove or disprove that selected stars or groups of stars belong to the LMC or the SMC. As an example, we selected the objects which are located inside the classical Cepheid instability strip on CMD, did not show significant light variations in the OGLE-III data and have proper motions coherent with the LMC one. Additional observations will then allow empirical bounding of the instability strip.

**Acknowledgements.** Authors thank S. Kozłowski for comments on early draft and J. Chanamé for discussion. This work was supported by MNiSW grant N-N203-512538. RP was supported through Polish Science Foundation START program. The OGLE project has received funding from the European Research Council under the European Community's Seventh Framework Programme (FP7/2007-2013)/ERC grant agreement No. 246678.

## REFERENCES

- Alcock, C., *et al.* 2001, *ApJ*, **562**, 337.  
Anderson, J., and King, I.R. 2003, *AJ*, **126**, 772.  
Catalán, S., *et al.* 2008, *A&A*, **477**, 213.

- Chanamé, J., and Gould, A. 2004, *ApJ*, **601**, 289.
- Cioni, M.-R., *et al.* 2000, *A&AS*, **144**, 235.
- Eyer, L., and Woźniak P.R. 2001, *MNRAS*, **327**, 601.
- Farihi, J., Becklin, E.E., and Zuckerman, B. 2005, *ApJS*, **161**, 394.
- Fedorov, P.N., Myznikov, A.A., and Akhmetov, V.S. 2009, *MNRAS*, **393**, 133.
- Freire, P. C., *et al.* 2001, *MNRAS*, **326**, 901.
- Freire, P. C., *et al.* 2003, *MNRAS*, **340**, 1359.
- Girard, T.M., *et al.* 2011, *AJ*, **142**, 15.
- Graczyk, D., Soszyński, I., Poleski, R., Pietrzyński, G., Udalski, A., Szymański, M. K., Kubiak, M., Wyrzykowski, Ł., and Ulaczyk, K. 2011, *Acta Astron.*, **61**, 103.
- Holberg, J.B., and Bergeron, P. 2006, *AJ*, **132**, 1221.
- Jordan, S., *et al.* 1998, *A&A*, **330**, 277.
- Kallivayalil, *et al.* 2006a, *ApJ*, **638**, 772.
- Kallivayalil, N., van der Marel, R.P., and Alcock, C. 2006b, *ApJ*, **652**, 1213.
- Kinman, T.D., Cacciari, C., Bragaglia, A., Buzzoni, A., and Spagna, A. 2007, *MNRAS*, **375**, 1381.
- Kozłowski, S., Kochanek, C.S., Jacyszyn, A.M., Udalski, A., Szymański, M. K., Poleski, R., Kubiak, M., Soszyński, I., Pietrzyński, G., Wyrzykowski, Ł., Ulaczyk, K., and Pietrukowicz, P. 2012, *ApJ*, **746**, 27.
- Kuijken, K., and Rich, R.M. 2002, *AJ*, **124**, 2054.
- Makarov, V.V. 2012, *MNRAS*, **421L**, 11.
- Martin, J.C., and Morrison, H.L. 1998, *AJ*, **116**, 1724.
- Monteiro, H., *et al.* 2006, *ApJ*, **638**, 446.
- Odenkirchen, M., Brosche, P., Geffert, M., and Tucholke, H.J. 1997, *New Astronomy*, **2**, 477.
- Piatek, S., Pryor, C., and Olszewski, E.W. 2008, *AJ*, **135**, 1024.
- Pojmański, G. 1997, *Acta Astron.*, **47**, 467.
- Poleski, R., Soszyński, I., Udalski, A., Szymański, M. K., Kubiak, M., Pietrzyński, G., Wyrzykowski, Ł., and Ulaczyk, K. 2011, *Acta Astron.*, **61**, 199 (Paper I).
- Quinn, D.P., *et al.* 2009, *MNRAS*, **396**, 11.
- Sabogal, B.E., Mennickent, R.E., Pietrzyński, G., and Gieren, W. 2005, *MNRAS*, **361**, 1055.
- Schechter, P.L., Mateo, M., and Saha, A. 1993, *PASP*, **105**, 1342.
- Scholz, R.D., Szokoly, G.P., Andersen, M., Ibata, R., Irwin, M. J. 2002, *ApJ*, **565**, 539.
- Schönrich, R., Binney, J., and Dehnen, W. 2010, *MNRAS*, **403**, 1829.
- Sesar, B., Ivezić, Ž., and Jurić, M. 2008, *ApJ*, **689**, 1244.
- Sion, E.M., Oswalt, T.D., Liebert, J., Hintzen, P. 1991, *AJ*, **101**, 1476.
- Skrutskie, M.F., *et al.* 2006, *AJ*, **131**, 1163.
- Soszyński, I., Żebruń, K., Udalski, A., Woźniak, P.R., Szymański, M., Kubiak, M., Pietrzyński, G., Szewczyk, O., and Wyrzykowski, Ł. 2002, *Acta Astron.*, **52**, 143.
- Soszyński, I., Poleski, R., Udalski, A., Kubiak, M., Szymański, M. K., Pietrzyński, G., Wyrzykowski, Ł., Szewczyk, O., and Ulaczyk, K. 2008, *Acta Astron.*, **58**, 163.
- Soszyński, I., Udalski, A., Szymański, M. K., Kubiak, M., Pietrzyński, G., Wyrzykowski, Ł., Szewczyk, O., Ulaczyk, K., and Poleski, R. 2009a, *Acta Astron.*, **59**, 1.
- Soszyński, I., Udalski, A., Szymański, M. K., Kubiak, M., Pietrzyński, G., Wyrzykowski, Ł., Szewczyk, O., Ulaczyk, K., and Poleski, R. 2009b, *Acta Astron.*, **59**, 239.
- Tucholke, H.J. 1992, *A&A*, **93**, 293.
- Udalski, A. 2003, *Acta Astron.*, **53**, 291.
- Udalski, A., Szymański, M.K., Soszyński, I., and Poleski, R. 2008a, *Acta Astron.*, **58**, 69.
- Udalski, A., Soszyński, I., Szymański, M. K., Kubiak, M., Pietrzyński, G., Wyrzykowski, Ł., Szewczyk, O., Ulaczyk, K., and Poleski, R. 2008b, *Acta Astron.*, **58**, 89.
- Udalski, A., Soszyński, I., Szymański, M. K., Kubiak, M., Pietrzyński, G., Wyrzykowski, Ł., Szewczyk, O., Ulaczyk, K., and Poleski, R. 2008c, *Acta Astron.*, **58**, 329.
- van der Marel, R.P., Alves, D.R., Hardy, E., and Suntzeff, N.B. 2002, *AJ*, **124**, 2639.
- Yoo, J., Chanamé, J., and Gould, A. 2004, *ApJ*, **601**, 311.